

Data Processing

Data recorded by the BIOPAC was analyzed using MATLAB (The Mathworks Inc, Natick, MA, USA). A wavelet-based algorithm¹ was used to reliably identify the onset and peak of the QRS complex and the termination of the T-wave in the ECG even in the presence of motion artefact. Intervals between R-waves (RRI; Figure 1) were used to calculate heart rate (HR) after artefacts and ectopic beats were identified and removed from each time series by an automated procedure² with manual oversight. QT interval was calculated and corrected for HR (QTc) on an individual basis using a least squares fit of a power function.³ The thoracic impedance data was filtered using an adaptive filter^{4,5} to remove the influence of body movements and respiration on the cardiac signal by excluding components of the signal which were not related to the RRI. Figure 1 shows fiducial points on the impedance cardiogram and their relative timing to the ECG and cardiac cycle. The B-point in this signal was identified automatically using a linear extrapolation technique,⁶ allowing accurate timing of aortic valve opening.⁷ The X-point in this signal was identified by searching for maxima in a 100 ms Gaussian-weighted window of data, which spans the T-wave termination time in the ECG, allowing accurate timing of aortic valve closure.⁷

Pre-ejection period (PEP) was calculated as the interval between R-wave onset and the B-point (Figure 1).⁸ Left ventricular ejection time (LVET) was calculated as the interval between the B-point and the X-point (Figure 1) and systolic time ratio (STR) as the ratio between PEP and LVET. Stroke volume (SV) was estimated using Kubicek's formula:⁹

$$SV = \rho_b \cdot \frac{l^2}{Z_0^2} \cdot LVET \cdot \left. \frac{dZ}{dt} \right|_{\min}$$

where ρ_b is the resistivity of blood ($\Omega \cdot \text{cm}$), l is the height of the thoracic segment measured (cm), Z_0 is the basal thoracic impedance (Ω), and $\left. \frac{dZ}{dt} \right|_{\min}$ ($\Omega \cdot \text{s}^{-1}$) is the absolute value of the maximum rate of fall of thoracic impedance during systole (coinciding with the C point; Figure 1). We used a fixed

value of 135 Ω .cm for ρ_b in accordance with current guidelines which suggest that this yields more accurate results than individual correction of ρ_b for haematocrit.¹⁰

CO and SVR were derived from SV as follows (where MAP refers to mean arterial pressure):

$$CO = \frac{SV \cdot HR}{1000} \qquad SVR = 80 \cdot \left(\frac{MAP - CVP}{CO} \right)$$

We simplified the SVR equation to exclude the central venous pressure (CVP) term which is usually close to zero and unvarying.

To control for the potential confounding influence of associations between size at birth and body surface area (BSA), we calculated the indexed versions of the SV, CO, and SVR variables by dividing them by BSA. BSA was calculated using a method that has been validated in children.¹¹

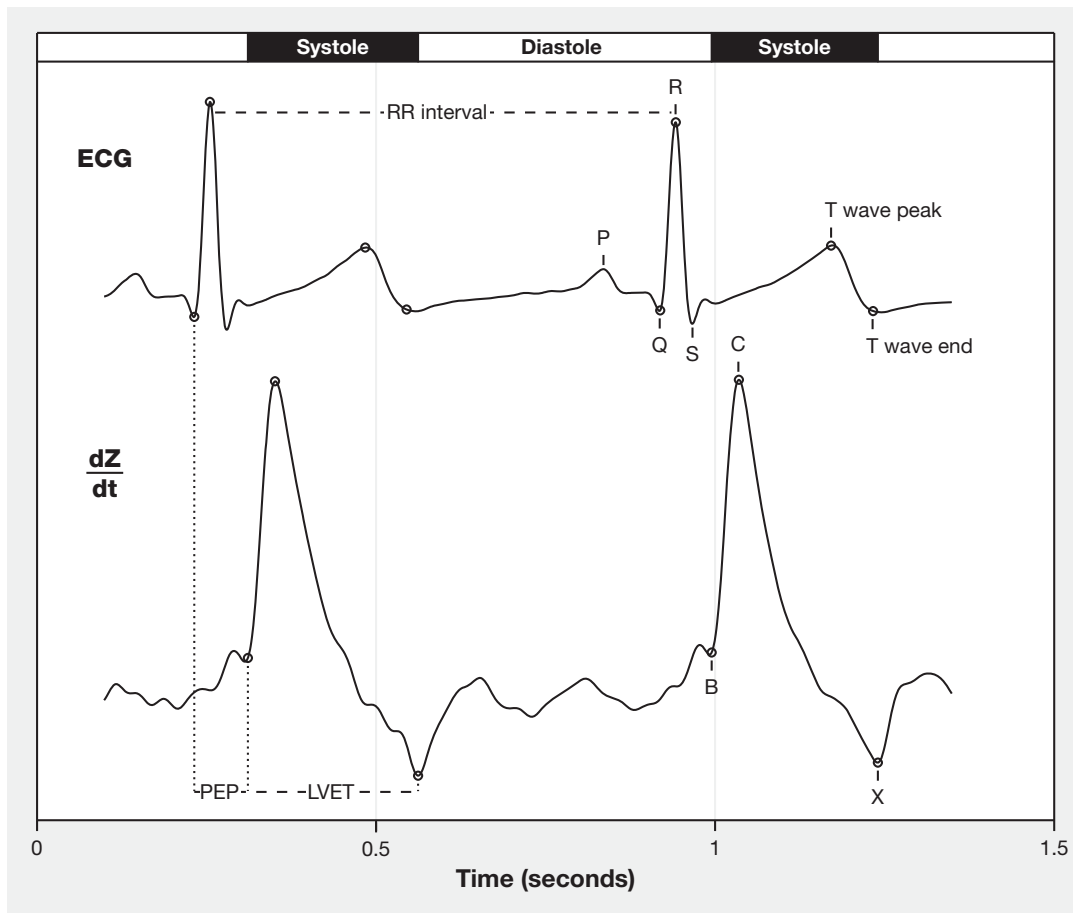


Figure 1. A representative recording of the electrocardiogram (ECG) and first time-derivative of the impedance cardiogram ($\frac{dZ}{dt}$) from a single study participant over two heart beats. Following convention, impedance is shown such that a decrease in impedance results in a greater y-axis magnitude. The cardiac cycle and the derivation of cardiac time intervals – RR interval, pre-ejection period (PEP) and left ventricular ejection time (LVET) – are indicated. Hollow circles indicate fiducial points on both signals identified automatically by computer. In addition to the well-known PQRST sequence of the ECG, major time points on $\frac{dZ}{dt}$ are marked. These include the B-point which coincides with opening of the aortic valve, the X-point which coincides with closure of the aortic valve, and the C-point which marks the maximum rate of decline in thoracic impedance which coincides with peak systolic ejection rate.

References

1. Martínez JP, Almeida R, Olmos S, Rocha AP, Laguna P. A wavelet-based ECG delineator: evaluation on standard databases. *IEEE Trans Biomed Eng* 2004;**51**:570-581.
2. Berntson GG, Quigley KS, Jang JF, Boysen ST. An approach to artifact identification: application to heart period data. *Psychophysiology* 1990;**27**:586-598.
3. Malik M, Färbom P, Batchvarov V, Hnatkova K, Camm AJ. Relation between QT and RR intervals is highly individual among healthy subjects: implications for heart rate correction of the QT interval. *Heart* 2002;**87**:220-228.
4. Barros AK, Yoshizawa M, Yasuda Y. Filtering Noncorrelated Noise in Impedance Cardiography. *IEEE Trans Biomed Eng* 1995;**42**:324-327.
5. Ono T, Yasuda Y, Ito T, Barros AK, Ishida K, Miyamura M, Yoshizawa M, Yambe T. Validity of the Adaptive Filter for Accurate Measurement of Cardiac Output in Impedance Cardiography. *Tohoku J Exp Med* 2004;**202**:181-191.
6. Ono T, Miyamura M, Yasuda Y, Ito T, Saito T, Ishiguro T, Yoshizawa M, Yambe T. Beat-to-beat evaluation of systolic time intervals during bicycle exercise using impedance cardiography. *Tohoku J Exp Med* 2004;**203**:17-29.
7. Lababidi Z, Ehmke DA, Durnin RE, Leaverton PE, Lauer RM. The First Derivative Thoracic Impedance Cardiogram. *Circulation* 1970;**41**:651-658.
8. Berntson GG, Lozano DL, Chen YJ, Cacioppo JT. Where to Q in PEP. *Psychophysiology* 2004;**41**:333-337.
9. Kubicek WG, Karnegis JN, Patterson RP, Witsoe DA, Mattson RH. Development and Evaluation of an Impedance Cardiac Output System. *Aerosp Med* 1966:1208-1212.

10. Sherwood A, Allen MT, Fahrenberg J, Kelsey RM, Lovallo WR, van Doornen LJ. Methodological guidelines for impedance cardiography. *Psychophysiology* 1990;**27**:1-23.
11. Haycock GB, Schwartz GJ, Wisotsky DH. Geometric method for measuring body surface area: a height-weight formula validated in infants, children, and adults. *J Pediatr* 1978;**93**:62-66.